2018 IEEE 16th Student Conference on Research and Development (SCOReD), Bangi, Malaysia (26-28 Nov 2018)

Superpixel Classification with Color and Texture Features for Automated Wound Area Segmentation

Topu Biswas[1], Mohammad Faizal Ahmad Fauzi[1], Fazly Salleh Abas[2] and Harikrishna K.R.Nair [3]
[1]Faculty of Engineering, Multimedia University, Malaysia
[2]Faculty of Engineering and Technology, Multimedia University, Malaysia
[3]Wound Care Unit, Department of Internal Medicine, Hospital Kuala Lumpur, Malaysia
Email: topu.bd00@gmail.com, {faizal1, fazly.salleh.abas}@mmu.edu.my, hulk25@hotmail.com

***Abstract*—Chronic wound is becoming a major threat for world health and economy. In the USA alone, an estimated 6.5 million people are affected by the chronic wound and the annual cost for chronic wound treatment is reportedly more than 25 billion dollars. The process of chronic wound healing is very complex and time-consuming. Quantification of wound size plays a vital role for clinical wound treatment as the physical dimension of a wound is an important clue for wound assessment. The current techniques for wound area measurement are the ruler method and tracing which is mainly based on visual inspection, thus are not very accurate as well as time-consuming. A computerized wound measurement system can provide a more accurate measurement, reduce bias and errors due to fatigue and can potentially reduce clinical workload. In this paper, we proposed a simple but efficient method for wound area segmentation based on superpixel classification with color and texture feature and SVM classifier. Some important findings throughout our experiment are also discussed.**

***Keywords*—*chronic wound; color histogram feature; local binary pattern; support vector machine (SVM); wound image segmentation; superpixel classification*.**

I. Introduction

Wound can be defined as the breakage of normal skin tissue due to violence, accident, or surgery. Based on the time needed for healing, wounds can be classified into two types: acute wound and chronic wound. As defined by the Centers for Medicare and Medicaid Services, chronic wounds are wounds that takes more than 30 days to heal. The duration for chronic wound healing varies from several months to several years [1]. As chronic wound takes a long time to heal, the treatment for the chronic wound is very costly and time-consuming. The cost for a single diabetic ulcer treatment is an estimated USD 5,0000 [2] and the total health care cost for the chronic wound is reportedly over USD 25 billion per year[3]. Due to the increasing rate of obesity and diabetic patient, the number of chronic wound patients is also increasing. In the USA alone, more than 6.5 million people are affected by chronic wound [4]. In developed countries, 1-2% of all population is affected by chronic wound during their lifetime [5]. Wound area measurement is an integral and objective component of wound assessment. In [6], the author explained the importance of accurate wound measurement for clinical wound treatment and also stated that the lack of accurate and objective wound measurement method is a major hindrance for wound assessment. As such, there is a need for a timely and accurate method for wound measurement in both the inpatient and outpatient settings.

The current clinical techniques for wound measurement are the ruler method and tracing based method which requires much human involvement and these methods mainly based on visual inspection [7]. They are also subject to intra and inter-reader variability. Fig. 1 illustrates the ruler-based wound measurement system. Literature reviews show that this method has an error rate up to 44% [8]. In Fig. 1(b) and 1(c) although the wound area is different but for the ruler method wound area will be same as their major axes lengths are same. In the tracing method, a square marked transparent foil placed on the wound and the wound boundary is marked using a pen. The wound area is measured by summing the square area which belongs to the traced wound boundary. Its accuracy is limited due to less contribution of squares which are located on the border of the wound. As showed in Fig. 2(b) the wound touches only a few portions of the square, but in tracing method, those square area will be counted as wound area. In computerized measurement system, this type of error will be resolved as it measures the wound pixel-wise. Some clinician's also using digital photography to trace the wound area. However, such an ad hoc method doesnt achieve comprehensive clinical benchmark. A computerized wound measurement system can potentially reduce human intervention, provides traceable clinical information and makes the treatment and care more consistent and accurate.

This paper is organized as follows: Section 2 presents literature review, In section 3 overall methodology of our proposed system is presented. Section 4 describes the results and important findings throughout our experiment. Finally, Section 5 concludes the paper along with some future works.

II. Related Work

Wound area segmentation from digital photography image was the subject matter of several researches. In [9] , the authors attempted to introduce a mobile application based on dynamic active contour model. They modified the active counter model by changing the energy calculation. They also applied some preprocessing technique to minimize errors from artifacts and lighting condition. They reported an accuracy of 90% but the method is sensitive to the viewing angle, lighting conditions

978-1-5386-9175-5/18/$31.00

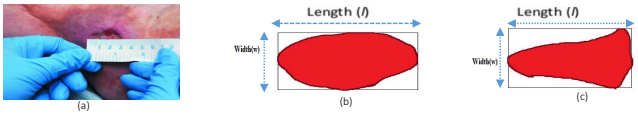

Fig. 1. Ruler Based Wound Measurement System [7].

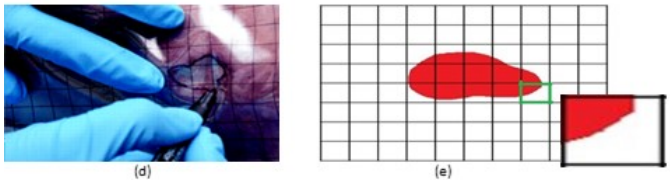

Fig. 2. Tracing Based Method Wound Measurement System [7].

and camera distance, which highly affect the usability of the proposed scheme. The authors in [10] proposed method based on the combination of neural network and Bayesian classifier. They used mean shift algorithm for smoothing raw images and later they used region growing method to segment wound region. In [11], the authors tried to find out best working color channel for wound area segmentation using mean contrast. They used Db and Dr Color channel to segment the wound area. Their algorithm with k-means and fuzzy c-mean were able to detect wound surface, but the accuracy not very high. In [12], probability map approach was proposed to determine wound boundary. But this approach is not fully automated and doesnt work accurately for black skin tone images. Wang et al. [13] proposed a two-stage SVM-Based system for wound area determination but this system requires an extra imaging device to capture the wound image. In [13], a semi-automated method based on fuzzy spectral clustering was introduced . This method needs a manual input of prototype number **C** and fuzzy similarity constructor **t**. In [14] and [15] the authors introduced deep learning based method for wound area segmentation. But this method requires high computational power.

Most of the methods discussed above require either high computational power, conditional image capture, partial human involvement.

III. Methodology

The wound images used for our experiment are provided by the Comprehensive Wound Center of the Ohio State University Wexner Medical Center, with Institutional Review Board (IRB) approval. The images were taken under uncontrolled imaging condition by medical center staff.

Fig. 3 depicts the overall methodology for the proposed wound area segmentation. To differentiate wound from the skin, color is the most important visual clue for the human eye. Along with color, texture also plays an important clue (see Fig. 4). In this research, we attempted a supervised machine learning approach with color and texture feature. To classify pixel one of the three class (wound, skin, and background), we proposed the two-step classification approach which we will discuss elaborately in later section.

The overall methodology can be divided into two parts: I) in training part, we trained SVM model for superpixel classification and II) in the testing part we used those model for wound area segmentation from a new wound image. For first (training) part of our methodology, we used a set of 100 images. First, we divided an input image into number of superpixels. A total of 47,718 superpixel region generated from all 100 images. After superpixel segmentation, we extracted color and texture feature form all superpixel region. The ground truths for wound area were provided by expert clinician of Ohio State University Wexner Medical Center and the ground truth of skin drawn by us. Based on this ground truth, superpixel features are labeled into three classes i.e., wound, skin, and background. The number of superpixels extracted from the background, wound and skin portion is 22741, 22549 and 2428 respectively. Using this labeled feature, we conduct training stage as follows:

In the first stage of classification, we aimed to delineate background. For this purpose, we grouped wound and skin superpixels in the same class (named as “skin” class) and the background is in another class (named as “background” class). So a total of 24997 superpixels grouped skin class and 224741 superpixels in background class. Then we split up all the samples into five folds of equal size. After then we followed the standard five-fold cross-validation scheme to train a binary classifier. In the second stage, after delineation background we have only two class, “skin” and “wound” and we trained an SVM classifier for those two class. In this stage of training, we also followed the five-fold cross-validation scheme as like the first stage.

In second part (testing) of methodology, we use the classification models (one is for classifying “background” and “skin” and another is for classifying “wound” and “skin”) obtained from first part. To segment wound area, we first perform superpixel segmentation for a new input image. Then we perform two stage classification for each superpixel. In first stage we check whatever it is “skin” or “background” class using first trained model. If “skin”, then it fed to second trained model to classify “skin” and “wound”, otherwise discard it. Based on the classifier response we obtained from the two stages, a segmented image is constructed. Finally, some morphological operation like hole filling, area base filtering also performed to refine the output image.

A. Superpixel Segmentation:

Superpixel can be defined as the group of connected pixels on an image which has similar characteristics. Our main goal is to develop a fully automated system which can segment wound area from photographic images, captured from the real clinical environment and without any controlled environment and taken by general people (not by a professional photographer). For this, some pixel of wound image may get corrupted or distorted due to motion blur, lighting condition etc. Other than a single pixel, a connected group of pixels gives more meaningful information about the specific image region. According

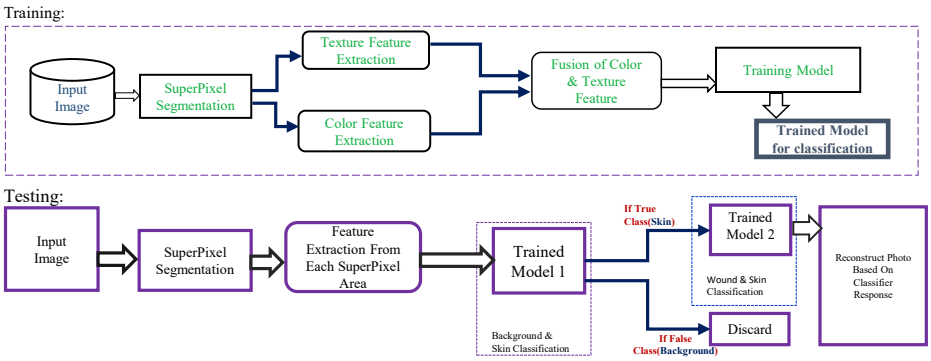

Fig. 3. Overall Methodology.

to the previous study and experiment, *Simple Linear Iterative Clustering* (SLIC) superpixel algorithm works well for our experiment. In [16], the authors compared SLIC superpixel segmentation with other superpixel segmentation algorithm and it indicates SLIC can correctly identify image boundary, while only needing low computational power to run.

In SLIC superpixel segmentation algoritm, first the original is RGB image converted to CIE Lab space to get of a good perceptual accuracy. Initially we need to input one parameter n, the approximate number of desired superpixel. SLIC algorithm puts n number initial clusters on the image. Then the cluster centers are replaced by the mean of all pixels distance in that cluster. For calculating distance from cluster center to other pixels on that cluster, SLIC superpixel consider color (L,A,B) and spatial (x,y) spaces. The distance calculation formula as below:

$$
\begin{aligned}
D_c &= \sqrt{\left(L_j - L_k\right)^2 + \left(A_j - A_k\right)^2 + \left(B_j - B_k\right)^2} \\
D_s &= \sqrt{\left(x_j - x_k\right)^2 + \left(y_j - y_k\right)^2} \\
D &= \sqrt{D_c^2 + \left(\frac{D_s}{S}\right)^2 m^2}
\end{aligned}
\tag{1}
$$

Here, L_j, A_j, B_j, x_j, y_j and L_j, A_j, B_j, x_j, y_j two points in 5-D color and spatial space. S is the approximate superpixel size calculated by: S= (Image size/n). The parameter m is spatial proximity, using this we can give more or less weight on the spatial coordinate.

Supervised machine learning approach needs a lot of training samples to perform best. We divided our image dataset into training and testing datasets. For the training dataset, superpixel segmentation is carried out on all the images. The generated superpixels are used for training where suitable feature extraction will be applied. During the testing (segmentation) stage, the image is also applied the superpixel segmentation, except that the generated superpixels will be classified into either wound, skin or background based on the trained model.

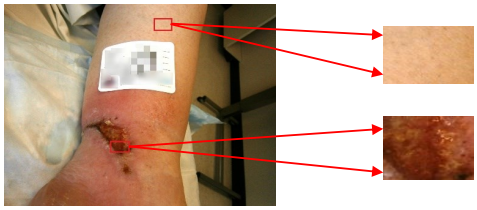

Fig. 4. Illustration of Texture Nature of Skin and Wound Region.

B. Color Feature Extraction:

For color feature, we used pixel- based color histogram feature. In a monochromic image, every pixel is represented by a single gray level intensity value. The intensity value lies between 0 and 255. A color image on the other hand is formed by three channels. A histogram measures the frequency of a given data values. In RGB color image in each channel intensity varies between 0 to 255 and the combination of this three gray intensity a new color is formed. To create a color feature, we separately counted histogram from every channel of an RGB image with 50 bins, after then concatenation of three channel we get our final feature of 150 bins. Fig. 5 shows a visual illustration of the histogram feature.

C. Texture Feature Extraction:

For texture features, we used the uniform Local Binary Pattern (LBP). For every pixels in the image, we consider their 3x3 neighbors. The center pixels are compared to their 8 neighbors: if the center pixel's value is greater than the neighbor's value, that neighbors value is changed to "0", otherwise, it is changed to "1". This gives 8-bit binary numbers

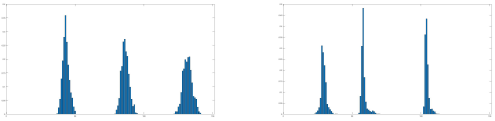

(a) For a Skin Superpixel (b) For a Wound Superpixel

Fig. 5. Visual Illustration of Superpixel Histogram.

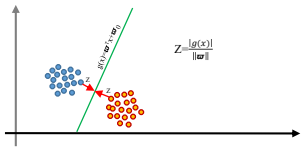

Fig. 6. Illustration of SVM Hyperplane.

for the neighbors, which are then converted into decimals. Finally histogram computation is performed to get the basic LBP feature. For given a pixel at (x_c, y_c), the resulting LBP can be expressed in decimal form as:

$$LBP_{P,R}(x_c, y_c) = \sum_{P=o}^{P-1} S(i_p - i_c)2^p \tag{2}$$

$$s_k = \begin{cases} 1 & x \geq 0 \\ 0 & x < 0 \end{cases} \tag{3}$$

Where the notation (P, R) denotes a neighborhood of P sampling points on a circle of radius of R. The above LBP operator gives 2^p output value for a number of P neighbor. If the image is rotated, the surrounding pixels in every neighbor pixel will also rotate along the perimeter. This generates different LBP value. To make LBP rotational effect free, rotational invariant LBP is proposed in [17].

$$LBP^{ri}_{P,R} = min\{ROR(LBP_{P,R}, i) \mid (i = 1, 2, 3...P-1)\} \tag{4}$$

Where, $ROR(x, i)$ accomplishes a circular bit-wise right shift on the P-bit number. It has been presented in [17], certain pattern gives more meaningful information about texture than rotational-invariant LBP and it can be possible by taking a subset value of 2^p. Ojala et al. named these patterns uniform patterns. As we discussed earlier, every center pixel gives 8-bit binary pattern, if this pattern holds at most two bitwise transitions from 0 to 1 or 0 to 1 then, it is denoted as uniform. For example: 00001100 (2 transitions) is uniform and 10101001 (5 transitions) is not uniform. This uniform pattern reduces histogram bean from 256 to 59.

D. Support Vector Machine(SVM) Classifier:

For classification purpose we used Support Vector Machine (SVM) classifier. SVM generates a hyperplane or a set of hyperplanes in a high or infinite-dimensional space based on the training samples. The best choice of hyperplane will be those hyperplane which keeps maximum distance from both classes (Fig. 6). Using this hyperplane SVM can classify new (test) cases. In our two-stage approach, the SVM is first used to separate the background from the skin and wounds. In the second stage, it is used to separate the skins from the wounds.

IV. Result & Discussion

As discussed above, our methodology is a combination of two parts that are classification and segmentation. In the first part of our methodology we will discuss the classification result and after then we will present the segmentation result.

Fig. 7. Confusion Matrix for first stage of classification.

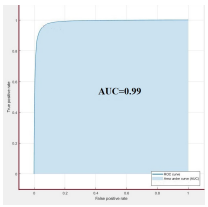

Fig. 8. Receiver operating characteristic (ROC) curve for first stage classification .

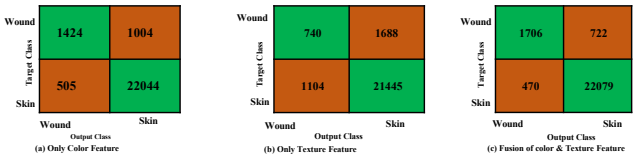

Fig. 9. Confusion matrix for second stage of classification.

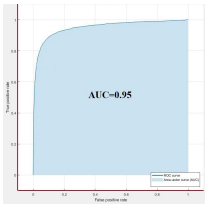

Fig. 10. Receiver operating characteristic (ROC) curve for second stage classification .

A. Superpixel Classification:

In our methodology, we proposed two-stage classification approach to classify background, skin and wound. The first stage classification is performed is to classify "skin" and "background". In stage "skin" and "wound" classification is performed. The accuracy, sensitivity, and specificity computed based on the following formulas:

$$Accuracy = \frac{TP + TN}{TP + TN + FP + FN} \tag{5}$$

$$Sensitivity = \frac{TP}{TP + FN} \tag{6}$$

$$Specificity = \frac{TN}{TN + FP} \tag{7}$$

Where, TP=True Positive, TN=True Negative, FP=False Positive, and FN=False Negative.

TABLE I: First Stage Classification Result.

Feature	Accuracy	Sensitivity	Specificity
Only Color	92.7%	94.75%	90.55%
Only texture	79.0%	81.22%	76.64%
Fusion of Color & Texture	95.0%	95.99%	93.88%

TABLE II: Second Stage Classification Result.

Feature	Accuracy	Sensitivity	Specificity
Only Color	94.0%	58.65%	97.76%
Only texture	88.8%	30.47%	95.10%
Fusion of Color & Texture	95.2%	70.26%	97.92%

Skin and Background Classification (First Stage): The result of skin and background classification showed in Table 1. We experiment for only color feature, only texture feature, and fusion of color and texture feature. As we can see from the truth table shown in fig.7, for skin superpixel classification the classification result for only color feature seems good but overall fusion of color and texture feature perform best. The overall accuracy for skin classification 95.0% using fusion of color and texture feature.

Skin and Wound Classification (Second stage): After delineation of background, the objective of this stage is to classify fine skin and wound. The result for this stage shown in Table 2. For skin and wound classification, we can observe the overall accuracy using only color feature and using the fusion of color and texture feature is nearly similar. But when we look over on the truth table. We can observe the color feature alone not good for the classification wound superpixel. The sensitivity for wound detection using only color feature is only 58.65% and fusion of color and texture feature it increases up to 70.26%.

As we see from the confusion matrix for both stages although the overall accuracy is good but the wound superpixel detection isn't so satisfactory. We observed, the superpixel of wound that is from granulation (red tissue) is most of the cases correctly classified and the classification rate for slough (yellow tissue) and eschar (black tissue) is not good. The image used our experiment, most of the portion of that contains background and skin. So the wound sample is less and within that, we also observed the number of slough and eschar sample is very few. In the next stage of our research, we intend to gather a number of wound sample which bears all types of wound properties.

B. Segmentation:

This work is the continuation of the previous research [12]. In previous research, the proposed method was not fully automated. In this stage of research, we intend to develop a fully automated system for wound area segmentation and in this paper, we reported the primary part of that, mainly focused on robust feature exploration for superpixels classification which is extracted from a different portion of a wound image. Nevertheless, we test a new set of 10 images (other than the images used in the classification stage) for the segmentation result. To evaluate the segmentation accuracy the Jaccard index was calculated. Other than that Dice coefficient and classification rate was also calculated.

$$J(C,D) = \frac{C \cap D}{C \cup D} \tag{8}$$

Dice coefficient can be defined as follows:

$$D(C,D) = \frac{2 \times (C \cup D)}{|C| + |D|} \tag{9}$$

Where C and D indicate the computer segmented wound area and doctor's ground-truth. As our aim is to classify wound pixel correctly as well as to delineate skin and background pixel. To determine how many pixels are correctly classified another performance matrix also calculated, called classification rate. Classification rate can be simply defined as the ratio of a total number of correctly classified pixel to a total number of pixels contain the image.

The result for segmentation is around 72% and which seems promising as literature shows that the average agreement between clinicians varies between 67.4 to 84.3% [12]. Without any human involvement, to segment wound from the background is quite difficult task because sometimes skin and wound poses similar visual properties and the images we used for our experiment introduces very challenging characteristics because of complicated background, especially those red, yellow and black, interrupts the segmentation. Some results for segmentation shown in Fig. 11.

As we mentioned earlier, It is the continuation of previous research [12] in which computer need a manual input to identify wound region and the accuracy for wound segmentation 75.10%. Our proposed method in this paper is fully automated and the accuracy for wound area segmentation is 71.98%.

TABLE III: Segmentation Result.

Jaccard index	Dice coefficient	classification rate
71.98%	83.30%	98.91%

Some other method available in literature claimed better result for wound area segmentation but most of them are limited to various conditional settings whereas our proposed method is: I) fully automated that minimizes the clinicians initial involvement, II) computationally efficient, can be run on a simple smartphone that enables to take care patient from home, even they can easily contact with an expert clinicians under telemedicine framework, III) our system is trained with the images, taken in uncontrolled environment(lightning condition or camera angle etc.) that indicates versatile usability to common people and IV) the image used in our experiment, contains different types of complex environmental background that expands our system to use in a real clinical environment (no extra arrangement needed for wound image capture).

V. Conclusion

We have proposed a fully automated wound area segmentation based on fusion of color-texture feature. The feature

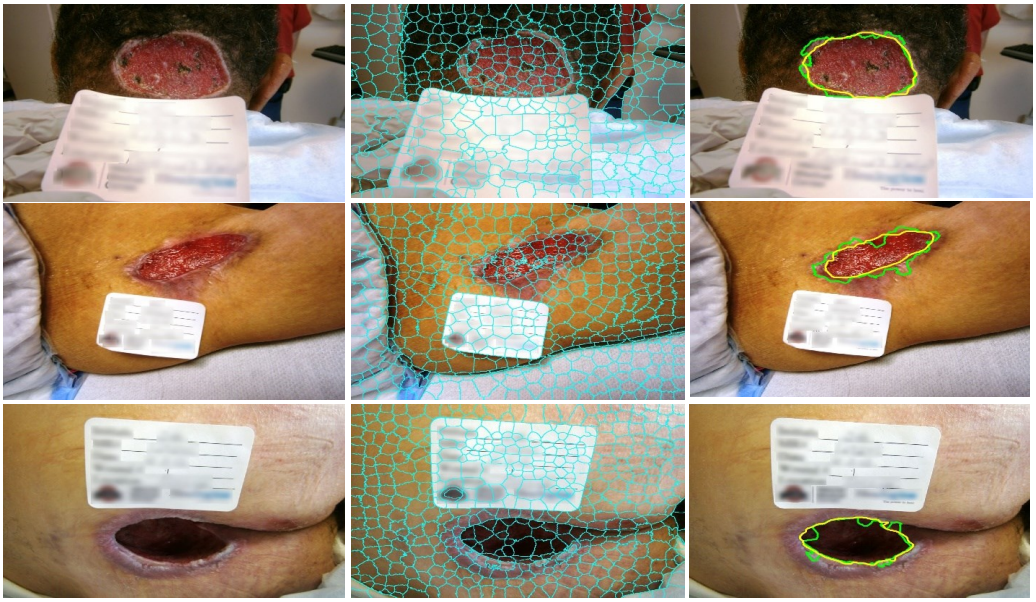

(a) Input Image (b) Superpixel Segmentation (c) Wound Segmentation (Green line indicates the computer segmented result & Yellow line indicates doctor ground truth

Fig. 11. Selected Segmentation Result .

extraction for this method is very simple and computationally efficient. The accuracy achieved for classification and segmentation seems promising compared to other work available in literature. The potency of this method discussed with different type of performance metrics. Our future aim is to explore with more enhanced set of data (which contains granulation, slough and eschar, all these three types wound) and more color and texture feature.

ACKNOWLEDGMENT

This research was fully funded by the Ministry of Science, Technology, and Innovation (MOSTI), Malaysia [Project Number 01-02- 01-SF0267]. We would like to thank our medical collaborators: Ohio State University Wexner Medical Center and Hospital Kuala Lumpur (HKL) for providing the database for this research and for their useful comments.

REFERENCES

[1] A. Lanau Roig, N. Fabrellas, G. Sáez Rubio, and K. Wilson, "Time of chronic wound healing, as part of a prevalence and incidence study," *Enfermería Global*, vol. 16, no. 46, pp. 445–463, 2017.

[2] H. George and C. Roger, "Chronic wound healing a review of current management and treatments," *Advances in therapy*, vol. 34, no. 3, pp. 599–610, 2017.

[3] H. Brem, O. Stojadinovic, R. F. Diegelmann, H. Entero, B. Lee, I. Pastar, M. Golinko, H. Rosenberg, and M. Tomic-Canic, "Molecular markers in patients with chronic wounds to guide surgical debridement," *Molecular medicine*, vol. 13, no. 1-2, p. 30, 2007.

[4] A. J. Singer and R. A. Clark, "Cutaneous wound healing," *New England journal of medicine*, vol. 341, no. 10, pp. 738–746, 1999.

[5] F. Gottrup, "A specialized wound-healing center concept: importance of a multidisciplinary department structure and surgical treatment facilities in the treatment of chronic wounds," *The American journal of surgery*, vol. 187, no. 5, pp. S38–S43, 2004.

[6] P. Plassmann, J. Melhuish, K. Harding *et al.*, "Methods of measuring wound size: a comparative study," *Wounds*, vol. 6, no. 2, pp. 54–61, 1994.

[7] J. E. Grey, K. G. Harding, and S. Enoch, "Abc of wound healing: pressure ulcers," *BMJ: British Medical Journal*, vol. 332, no. 7539, p. 472, 2006.

[8] R. A. Clark, K. Ghosh, and M. G. Tonnesen, "Tissue engineering for cutaneous wounds," *Journal of Investigative Dermatology*, vol. 127, no. 5, pp. 1018–1029, 2007.

[9] N. Hettiarachchi, R. Mahindaratne, G. Mendis, H. Nanayakkara, and N. D. Nanayakkara, "Mobile based wound measurement," in *Point-of-Care Healthcare Technologies (PHT), 2013 IEEE*. IEEE, 2013, pp. 298–301.

[10] F. Veredas, H. Mesa, and L. Morente, "Binary tissue classification on wound images with neural networks and bayesian classifiers," *IEEE transactions on medical imaging*, vol. 29, no. 2, pp. 410–427, 2010.

[11] M. K. Yadav, D. D. Manohar, G. Mukherjee, and C. Chakraborty, "Segmentation of chronic wound areas by clustering techniques using selected color space," *Journal of Medical Imaging and Health Informatics*, vol. 3, no. 1, pp. 22–29, 2013.

[12] M. F. A. Fauzi, I. Khansa, K. Catignani, G. Gordillo, C. K. Sen, and M. N. Gurcan, "Computerized segmentation and measurement of chronic wound images," *Computers in biology and medicine*, vol. 60, pp. 74–85, 2015.

[13] D. M. Dhane, M. Maity, T. Mungle, C. Bar, A. Achar, M. Kolekar, and C. Chakraborty, "Fuzzy spectral clustering for automated delineation of chronic wound region using digital images," *Computers in biology and medicine*, vol. 89, pp. 551–560, 2017.

[14] F. Li, C. Wang, X. Liu, Y. Peng, and S. Jin, "A composite model of wound segmentation based on traditional methods and deep neural networks," *Computational Intelligence and Neuroscience*, vol. 2018, 2018.

[15] C. Wang, X. Yan, M. Smith, K. Kochhar, M. Rubin, S. M. Warren, J. Wrobel, and H. Lee, "A unified framework for automatic wound segmentation and analysis with deep convolutional neural networks," in *Engineering in Medicine and Biology Society (EMBC), 2015 37th Annual International Conference of the IEEE*. IEEE, 2015, pp. 2415–2418.

[16] R. Achanta, A. Shaji, K. Smith, A. Lucchi, P. Fua, S. Süsstrunk *et al.*, "Slic superpixels compared to state-of-the-art superpixel methods," *IEEE transactions on pattern analysis and machine intelligence*, vol. 34, no. 11, pp. 2274–2282, 2012.

[17] T. Ojala, M. Pietikainen, and T. Maenpaa, "Multiresolution gray-scale and rotation invariant texture classification with local binary patterns," *IEEE Transactions on pattern analysis and machine intelligence*, vol. 24, no. 7, pp. 971–987, 2002.